# Implications of noise and neural heterogeneity for vestibulo-ocular reflex fidelity.

Timothy M. Hospedales* [1], Mark C.W. van Rossum [1], Bruce P. Graham [2] and Mayank B. Dutia [3]

[1] Institute for Adaptive and Neural Computation, School of Informatics, University of Edinburgh, 5 Forrest Hill, Edinburgh EH1 2QL, UK

[2] Department of Computing Science and Mathematics, University of Stirling, Stirling FK9 4LA, UK

[3] Centre for Integrative Physiology, School of Biomedical Sciences, University of Edinburgh, Hugh Robson Building, George Square, Edinburgh EH8 9XD, UK

***Corresponding author:** Timothy M. Hospedales, Institute for Adaptive and Neural Computation, School of Informatics, University of Edinburgh, 5 Forrest Hill, Edinburgh EH1 2QL, UK

Email: t.hospedales@ed.ac.uk

**Keywords:** vestibular, network, oculomotor, population code, synchrony

**Acknowledgements:** TMH is supported by an EPSRC/MRC Scholarship to the Doctoral Training Centre in Neuroinformatics. Research in the laboratory of MBD is supported by the Wellcome Trust, BBSRC and EPSRC.

**Abstract**

The vestibulo-ocular reflex (VOR) is characterised by a short-latency, high fidelity eye-movement response to head rotations at frequencies up to 20Hz. Electrophysiological studies of medial vestibular nucleus (MVN) neurons however show that their response to sinusoidal currents above 10 -12Hz is highly non-linear and distorted by aliasing for all but very small current amplitudes. How can this system function *in vivo* when single cell response cannot explain its operation? Here we show that the necessary wide VOR frequency-response may be achieved not by firing-rate encoding of head velocity in single neurons, but in the integrated population response of asynchronously-firing, intrinsically active neurons. Diffusive synaptic noise and the pacemaker-driven, intrinsic firing of MVN cells synergistically maintain asynchronous, spontaneous spiking in a population of model MVN neurons, over a wide range of input signal amplitudes and frequencies. Response fidelity is further improved by a reciprocal inhibitory link between two MVN populations, mimicking the vestibular commissural system *in vivo,* but only if asynchrony is maintained by noise and pacemaker inputs. These results provides a previously missing explanation for the full range of VOR function and a novel account of the role of the intrinsic pacemaker conductances in MVN cells. The values of diffusive noise and pacemaker currents that give optimal response fidelity yield firing statistics similar to those *in vivo*, suggesting that the *in vivo* network is tuned to optimal performance. While theoretical studies have argued that noise and population heterogeneity can improve coding, to our knowledge this is the first evidence indicating that these parameters are indeed tuned to optimize coding fidelity in a neural control system *in vivo.*

## 1. Introduction

A number of recent analytical and computational modelling studies have considered the signal processing characteristics of neuronal populations, and the effects of spontaneous spiking activity on the population response (Knight, 1972; Gerstner, 2000; van Rossum et al, 2002; Masuda & Aihara 2003, Masuda et al, 2005). These studies have revealed that the population response of a set of tonically active, asynchronously firing neurons can encode a common input signal with high fidelity and linearity over a wide operating range. Moreover the population response to changes in synaptic input is virtually immediate, since at any given time there is always a subset of neurons that are near firing threshold. This contrasts with the population response of neurons lacking tonic spiking activity, where changes in input will either evoke no response if they are too small or generate a response with a certain integration latency and a tendency towards synchronicity and periodicity, over a relatively restricted linear range (e.g. Diesman et al., 1999). However, the question which of these codes are used in sensory systems is difficult to address in pathways that have extensive downstream processing, which could extract different aspect of the activity. Therefore we researched this issue in a relatively simple system, the brainstem horizontal vestibulo-ocular reflex (hVOR) pathway (Fig. 1), which routes sensory input almost directly to the motor output, without any subsequent processing.

The hVOR pathway has been extensively investigated experimentally (Huterer & Cullen 2002, Minor et al., 1999, Ramachandran & Lisberger 2006, 2007) and many analytical and cellular models exist (Cartwright and Curthoys 1996; Arnold and Robinson 1997; Graham and Dutia 2001; Cartwright et al., 1999, 2003). Neurons in the medial vestibular nucleus (MVN; Type I neurons, Fig. 1) play a key role in transforming head-velocity inputs from horizontal semicircular canal afferents into motor commands to the abducens and oculomotor nuclei, which generate compensatory eye movements and stabilize gaze. The MVNs of the two sides are linked by a reciprocal inhibitory commissural pathway involving Type II inhibitory interneurons (Fig. 1), which is essential for the normal gain and time-constant of the hVOR. While additional pathways including the cerebellar flocculus are necessary for gain calibration and adaptive control of the VOR, the essential circuitry in Fig. 1 represents the core VOR pathway that mediates on-line feed forward eye movement responses to head rotation in the horizontal plane.

Experimental studies of MVN neurons in slices have shown that these neurons are intrinsically active, with pacemaker-like membrane conductances that generate a regular, spontaneous resting discharge *in vitro* (review, Straka et al 2005). Comparison of the *in vitro* and *in vivo* activity of MVN neurons in rodents shows that the spontaneous firing of MVN cells in slices is about 50% of their firing rate *in vivo* (Ris and Godaux, 1998). It is now widely accepted that the *in vivo* spiking activity of MVN neurons is the result of the interaction between their basal spontaneous pacemaker-driven firing and the excitatory and inhibitory synaptic inputs they receive from various sources. Computational (Av-Ron and Vidal 1999) and slice (du Lac and Lisberger 1995; Ris et al., 2001) studies of single MVN neuron response in rodents have reported a limited range of frequencies and amplitudes of input for which single neuron response is linear and follows the input accurately.

*In vivo* experiments in the monkey show that the VOR is linear, has a very short latency and is accurate up to 20 Hz (Huterer and Culleen 2002) and beyond (Ramachandran 2005). Assuming similar response properties for rodent and monkey neurons, single neuron responses can thus not account for the behavioural responses. Some recent studies have included realistic neurons in cellular network models (e.g. Cartwright et al., 1999, 2003). These models have not however included the intrinsic activity of MVN neurons, and do not account for the full range of real world VOR performance.

Because the pacemaker currents in each individual MVN neuron are independent, their mean rates are heterogeneous and hence timing of spiking activity in the population of MVN neurons is likely to be largely asynchronous. Additional factors promoting asynchronous firing in MVN neurons include the independent timing of spiking activity in their main excitatory input from vestibular nerve afferents, and in the inhibitory inputs they receive from interneurons in the vestibular commissural system (Fig. 1). Collectively the fluctuations from such independent synaptic inputs have been termed integration or diffusive noise (Gerstner, 2000). Here we investigate the hypothesis that diffusive noise and the intrinsic spontaneous activity of MVN hVOR neurons, by enhancing asynchrony in MVN population activity, enable the high fidelity linear response of the hVOR.

## 2. Model

### 2.1 Simulation Design

We simulated a population of 500 integrate and fire neurons, representing Type I MVN neurons receiving a common vestibular input e.g. from horizontal semicircular canal afferents (Fig. 1), and measured their population response and synchrony under various conditions. For the purpose of this study we employed a generic population of homogenous neurons which had an input resistance $R_m$= 100MΩ, a membrane time constant $\tau_m$= 20ms, a resting potential $E_{rp}$= -60mV, firing threshold $V_{th}$= -50mV, and 1ms absolute refractory period. The membrane potential for neuron $i$, $V_i$, evolved according to,

$$\tau_m \frac{dV_i(t)}{dt} = E_{rp} - V_i(t) + R_m\left(I(t) + P_i + \varepsilon_i(t)\right)$$

$$I(t) = I_0 + i(t) \quad P_i = N(\mu, \sigma_2) \quad \varepsilon_i(t) = N(0, \sigma_1)$$

To model potentially diverse spontaneous activity, a constant "pacemaker" current, $P_i$ for each neuron was chosen independently from a Gaussian distribution, $N(\mu, \sigma_2)$. Diffusive noise was simulated by independently injecting each neuron with low-pass filtered Gaussian noise, $\varepsilon_i(t)$ with a 2ms time-constant. The vestibular input signal $I(t)$ is directly injected to all neurons simultaneously. The resting input level $I_0$ simulated the steady input from vestibular afferents in the head-stationary condition, while dynamic input from head movement acts via $i(t)$. At initialization, the membrane potentials of the MVN neurons were assigned random values between $E_{rp}$ and $V_{th}$ from a weighted distribution calculated to give a stable spontaneous population activity over time as described in detail by van Rossum (2001). To further ensure the forgetting of initial conditions, in each simulation the population activity was allowed to settle for two seconds under constant resting input ($i(t)=0$), before application of a dynamic input signal and recording of results. In simulations where diffusive noise $\varepsilon(t)$ was kept at zero, the noise standard deviation was annealed down from an initial value of $\sigma_1$ =5pA to zero during the first second after initialization.

**2.2 Analysis of the population response to head-velocity inputs**

The population response to input was obtained by binning the spikes of all the neurons in the population into 5ms fixed width bins over the duration of the simulation (where 5ms bin size is chosen to correspond to the typical post-synaptic integration time). The input current stimulus was also binned into corresponding 5 ms bins. To quantify the fidelity of signal transmission, the mean absolute difference between the input and output bins was calculated over the simulation period, after normalizing the input current and output spikes relative to their own variance. Fidelity of signal transmission was expressed as one minus the mean error over the simulation period, with the maximum value of 1 corresponding to a perfect match between input and output bins. The population response is an appropriate representation for the output of this pathway as there are no further interneuron layers to decode any potential complex population code since MVN neurons converge directly on abducens motoneurons.

An alternative performance measure for sinusoidal signals consists of fitting sinusoids to both the input and output and evaluating their relative gain and phase difference (Ramachandran & Lisberger, 2006). However, our non-parametric fidelity measure is sufficient insofar as if either either are gain or phase are distorted, fidelity will also be degraded. Moreover, it is particularly appropriate here as we will evaluate the performance under more natural noisy multi-frequency input for which sinusoid fitting is inappropriate.

The degree of synchrony in the population of MVN neurons over the simulation period was quantified using a variant of the synchronization index of Burkitt & Clark (2001; Goldberg & Brow 1969). Each of N neurons defines a unit length vector of phase angle ($a_i$) determined by the position of its current membrane potential ($V_i$) in the range between resting potential and firing threshold:

$$a_i = \frac{2\pi V_i}{V_{th} - E_{rp}}$$

$$s = \sqrt{\left(\sum \cos(a_i)/N\right)^2 + \left(\sum \sin(a_i)/N\right)^2}$$

The mean vector of the population distribution is calculated, the magnitude of which defines a synchronization index ($s$) between one and zero. If all the neurons have the same membrane potential and hence phase angles, their unit vectors align and the magnitude of the population mean vector tends toward 1. Alternatively, if the neurons have a uniform

distribution of membrane potentials, their unit vectors are uniformly distributed in phase and the magnitude of the population mean vector therefore tends to zero. A synchronization index of 1 thus represents perfect synchronization of state, while an index of 0 represents uniform distribution of neural states and complete asynchrony. Population asynchrony is defined as one minus the synchronization index *s*. Given this instantaneous measure of synchrony, the synchrony for an entire simulation was simply defined as the mean of the index over all time steps. Alternate synchronization measures compute the phase alignment between spikes and a sinusoidal input, e.g. Ramachandran & Lisberger, 2006. In contrast, our measure essentially evaluates the probability distribution over membrane potentials in the population, with a uniform distribution corresponding to perfect asynchrony and a delta function distribution corresponding to perfect synchrony. This is motivated by the finding that fast, efficient population rate code transmission occurs in the domain when the distribution over membrane potentials is more uniform than peaked (van Rossum et al., 2002). Our procedure generalizes spike based measures, since correlated spikes occur as as the immediate result of correlated membrane potentials. The benefits of this measure are that synchrony can be quantified in response to non-periodic input as well as under conditions of few or no spikes where, for example, the entire population may be silent or refractory.

## 3. The independent effects of diffusive noise and pacemaker activity on the population response

### 3.1 Population response rate coding

To parametrize our model we use data from the alert monkey (Chen-Huang et al., 1997) in which a population of vestibular Type I cells were observed to fire with rate (62±33) Hz and with mean inter spike interval coefficient of variation (CV) of 0.29. We assume the variability in the mean rate to be due to heterogeneous innervation and pacemaker conductance strength. (However, the source of the heterogeneity does not matter for our purposes and we model these effects together). The firing irregularity is assumed to be due to diffusive noise effects.

To separate the effects of diffusive noise and pacemaker activity on population response, we created four model variants. The most realistic model variant (Model 3) included both diffusive noise and heterogeneous pacemaker activity. The parameters ($I_0$=115 pA, $\mu$=100

pA, $\sigma_1$=60 pA, $\sigma_2$=67 pA) were chosen such that the population had resting firing statistics matching those observed *in vivo* as described above. The next model variant (Model 2) included heterogeneous pacemaker activity but not diffusive noise by setting $\sigma_1$=0 pA which eliminated irregularity in individual neurons firing rate. Model 1 included the effects of the diffusive noise input, but in a homogeneous population, by setting $\sigma_2$=0 pA. Finally, Model 0 was a population of homogeneous noiseless neurons with ($I_0$=115 pA, $\mu$=100 pA, $\sigma_1$=0 pA, $\sigma_2$=0 pA).

The resting statistics before driven input are shown in Fig. 2(left) and population activity in response to a sample input in Fig. 2(right). In all four models the neurons initially fired asynchronously, with population synchrony s<0.25, because of their random initialization. The neurons in Model 0 (Fig. 2A) initially fired regularly, and at the same mean discharge rate, reflecting their identical pacemaker current inputs and lack of diffusive noise. In Model 1 the neurons initially fired less regularly due to the effects of the diffusive noise input $\varepsilon_i(t)$, but had similar average firing rates since they received the same pacemaker current injection $P_i$ (Fig. 2B). By contrast, the neurons in Model 2 initially discharged regularly because of the lack of diffusive noise, but at different average rates because each neuron received an independently selected amplitude of pacemaker current. The neurons in Model 3 fired irregularly, and at different average rates because they received both diffusive noise and heterogeneous pacemaker currents (Fig. 2D).

A driving input containing sinusoids of increasing amplitude and frequency was next applied (Fig. 2E). In response to the smallest input sinusoid (60pA, 4Hz), all four models generated a population response which represented the input fairly well. However, in response to the next input sinusoid (80pA, 10Hz), the neurons in Model 0 rapidly synchronized and the population response no longer represented the input signal. The synchronous firing continued even after the end of the sinusoidal input (Fig. 2A, arrows). By contrast, the neurons in Models 1 and 2 showed much greater resistance to synchronization, and the population response showed a good sinusoidal modulation over amplitudes and frequencies of input. In response to the the final input sinusoid (100pA, 16Hz), however, Model 1 again showed a small tendency to synchronize (Fig. 2B, arrows), suggesting that, for stronger driving inputs, the diffusive noise alone is less effective in resisting aliasing compared to the intrinsic pacemaker current inputs in Model 2. In Model 3, where the neurons received both diffusive noise and heterogeneous pacemaker current amplitudes, the

population response best followed the input signal over the sample amplitudes and frequencies.

To understand more clearly how the population rate code works, consider Fig. 3 which shows a more detailed segment of activity from the 500 cells in Model 0 and Model 3 configurations responding to the 16Hz frequency, 100pA amplitude input. Normalized instantaneous frequency (defined as $1/(t_2 - t_1)$, given spikes at times $t_1$ and $t_2$) is plotted against spike time along with the input in Fig. 3(top). In Fig. 3A, spikes from Model 0 (synchronization index, s=0.6) tend to occur synchronously with each other and at points phase locked with the input. (There are 150 overlapping spikes at only 25 unique times in this plot). There are extensive periods of input with no spikes at all during which downstream neurons have no information about the activity of the input. In Model 3 (Fig. 3B, s=0.14), the population's spike frequencies as a whole are modulated by the input much more smoothly in time and frequency. We also plot the population response based on 10 randomly selected cells (broken line) and of all 500 cells (unbroken line) for each model along with the input. In Model 0 the population response does not reflect the input well and this does not change significantly when considering 10 or 500 cells. This is because the synchronously firing cells are all firing at similar times, so adding further cells doing exactly the same thing carries no further information. In Model 3, because of the cells asynchronous firing times, the full 500 cell response reflects the input much more clearly than either the population response of a random 10 cell subset or an individual cell's instantaneous frequency. The signal is therefore not carried by the activity of any single cell, but by the mean rate of the whole asynchronous population, which allows transmission fidelity to increase with the number of cells.

### 3.2 Effects of input amplitude and frequency

Next, we quantified the performance of each model as a function of both input amplitude and frequency. Each model was simulated for 6s of driven sinusoidal input of fixed amplitude and frequency. The input frequencies were varied logarithmically between 0.5 and 20 Hz to emulate the physiological operating range of the mammalian (monkey) VOR (Huterer & Cullen 2002*)*. The amplitude $|i(t)|$ of the sinusoidal input was varied in 10pA steps between 10pA and 100pA. This caused modulations in firing frequency of the neurons from the barely significant at 10 pA to modulations of ±50Hz at 100pA, which was just small enough to avoid inhibitory 'cut-off' and silencing of the 62Hz resting rate during the contraversive half-

cycle of head rotation. For each model variant, the mean fidelity and synchrony over the course of each simulation are illustrated in Figure 4. In Model 0 (Fig. 4A) although the population is initialized randomly and asynchronously, it rapidly synchronizes in response to the input, particularly at the highest input frequencies and amplitudes. As a result, transmission fidelity for these inputs is poor. By contrast in Models 1 and 2, the diffusive noise input and pacemaker-current injection respectively are more effective in maintaining population asynchrony over the whole input range (Fig. 4B,C). However in Model 1 signal transmission fidelity falls off slightly at the highest amplitudes and frequencies (Fig. 4B, arrow). In Model 3, where the neurons receive both diffusive noise and pacemaker-current injection, synchrony is the lowest and signal transmission fidelity most robust throughout the input parameter space including the highest and lowest amplitudes and highest frequencies (Fig. 4D). In all cases, there is a reduced fidelity at the lowest amplitudes because the input-related response component becomes smaller with respect to stochastic fluctuations in the output, and hence the baseline error is increased compared to the higher amplitudes. The differences in performance between Model 0 and Models 1 – 3 illustrate the importance of asynchronous neuronal activity in maintaining population response fidelity over a wide range of input frequencies and amplitudes.

## 4. Continuous dependence of population response on the effects of diffusive noise and pacemaker activity

### 4.1 Sinusoidal Input

We wondered how the signal fidelity and population asynchrony depended on the exact amount of diffusive noise and the range of pacemaker currents. We measured the population response behaviour for three frequencies of vestibular input (Fig. 5). Three input signal frequencies were tested from the low, middle and high regions of the physiological range (0.5,8,20Hz) while the amplitude of the input signal was fixed at 100 pA (±50Hz firing rate modulation). The standard deviation of the diffusive noise input ($\sigma_1$) and pacemaker current heterogeneity ($\sigma_2$) were increased in 10 pA steps from 0 to 110 pA. This produced a range of simulations with resting statistics from zero CV and rate standard deviation to 0.46 CV and 51Hz rate standard deviation. Within this spectrum of parameters, the simulation equivalent to Model 0 lies at the origin of the plots. Models 1 and 2 lie along the y-and x-axes respectively. An interior point corresponds to the Model 3 configuration.

As expected, at low values of either diffusive noise or pacemaker current heterogeneity, the simulated neurons were prone to synchronization and signal transmission fidelity was poor. Particularly for the low input signal frequency of 0.5 Hz (Fig. 5A), even small additions of diffusive noise or pacemaker current heterogeneity resulted in a significant increase in the population asynchrony maintained and a corresponding large increase in fidelity. In the mid-frequency range (8 Hz, Fig. 5B) and the high-frequency range (20 Hz, Fig. 5C) fidelity again showed a rapid improvement with the addition of small to moderate levels of diffusive noise or pacemaker current heterogeneity. In both cases increasing pacemaker current heterogeneity was more effective and led to a steeper increase in fidelity, than the addition of diffusive noise. For each input frequency tested, there was a shallow peak of optimum transmission fidelity associated with a plateau in asynchrony in the mid-range values of diffusive noise and pacemaker current amplitudes (Fig 5, arrows). Beyond the optimum area of fidelity, the benefits of further increase in asynchrony were outweighed by progressively more noise driven, non-input related spiking. The distance from the origin of the peak region of transmission fidelity increased with input signal frequency (Fig. 5, arrows). Since the neural populations were more prone to synchronization in response to higher frequency inputs, higher values of diffusive noise and pacemaker current heterogeneity were required to obtain peak asynchrony and fidelity at high input signal frequencies (e.g. Fig. 5C vs. 5A).

### 4.2 Diffusive noise and pacemaker current levels yielding optimum population response to multiple-frequency input signals

Given the strong dependence of optimum tuning on input frequency, we investigated the levels of diffusive noise and pacemaker heterogeneity required for optimum response of the simulated MVN neurons to input of more biologically relevant statistics than pure sinusoids. To do this we constructed a random input signal with exponentially decaying (10ms time constant) power spectrum, similar to that observed for voluntary motion in monkeys (Huterer & Cullen, 2002). Fig. 6A illustrates the resulting fidelity surface for the the population. The best performing simulation – with best match between input and output population response - is at $\sigma_1$=50 pA, $\sigma_2$=50 pA (Fig. 6A, black arrow). The simulation with the most biologically realistic statistics (i.e. nearest to Model 3) is at $\sigma_1$=70 pA, $\sigma_2$=60 pA (Fig. 6A, white arrow).

As this is our analysis of main quantitative interest, we also increase the biological realism of the neurons incrementally. The adaptive properties of MVN neurons have been extensively

studied in the literature. In particular, they are known to exhibit post inhibitory rebound firing (PRF) and firing rate adaptation (FRA) (Straka et al 2005). We did not expect a strong quantitative effect as the time-constant of adaptation is on the order of one second, which is much longer than the time-constant of the input signal. For completeness, we nevertheless implemented these as described in detail by Sekirnjak and du Lac, (Sekirnjak and du Lac, 2002). Fig. 6B,C illustrate the fidelity and asynchrony surfaces for the adaptive population. In this case the highest fidelity simulation was at $\sigma_1$=60 pA, $\sigma_2$=50 pA (Fig 6B, black arrow).

In both cases the close match between the best performing simulation and the simulation best matching the biological statistics suggests that the *in vivo* system is broadly tuned to optimise transmission fidelity. As expected, the difference between the locations of the optimal adaptive (Fig. 6B) and non-adaptive (Fig. 6A) simulations was not large. The optimal adaptive simulation was slightly closer to the most realistic simulation. Every point on surfaces in Fig. 6A-C are averages over six independent simulations of 6s length after 2s of settling.

Sections of activity for the simulated adaptive neurons with low levels of diffusive noise and pacemaker current heterogeneity (Fig. 6B, first internal square. $\sigma_1$=10 pA, $\sigma_2$=10 pA) and for neurons in the optimal configuration are illustrated in Fig. 6D, E. In the low noise case the population response broadly followed the input signal but was markedly distorted by a tendency to synchronous bursting activity (arrows, Fig. 6D). By contrast, with moderate levels of diffusive noise and pacemaker current heterogeneity ($\sigma_1$=60 pA, $\sigma_2$=50 pA) the population response provided a much more faithful representation of the input signal (Fig. 6E).

**5. The commissural inhibitory system and population asynchrony in MVN neurons**

To investigate the contribution of the reciprocal commissural inhibitory connections between the bilateral MVNs (Fig. 1) on signal transmission, the simulations were repeated using two interconnected nuclei. The second nucleus was stimulated with the same mean input signal $I_0$ as the first, but with the dynamic component *i(t)* inverted. The nuclei are connected via Type II inter-neurons (Fig. 1) but we abstract their contribution by directly connecting the nuclei in an all-to-all manner and delaying spikes with the biologically observed 3ms latency delay. Synapses are modelled single exponential decay with 5ms time constant, approximating the

time constant *in vivo*. The resting $I_0$ input and synaptic strengths were scaled such that the firing rate of 62Hz with commissural inhibitory input was a 22% reduction of the spike rate that would otherwise be observed without the commissural connections (Ris & Godaux, 1998).

We compared the population responses of one MVN to sinusoidal head-velocity inputs with and without commissural inhibitory inhibition, using either a pair of MVNs with minimal diffusive noise ($\sigma_I$=5pA) or a pair of MVNs in the most biologically realistic Model 3 configuration. Using a single input frequency of 2Hz for clarity, Fig. 7 illustrates that the linking of two MVNs via a commissural inhibitory connection had a markedly deleterious effect on the response characteristics of low noise MVNs, but a beneficial effect on the response characteristics of the biologically realistic MVNs.

In the absence of the inhibitory commissural connection (Fig. 7A, dashed lines), the population response showed asynchrony and fair fidelity over a relatively restricted range of input signal amplitude, with a loss of asynchrony and drop in fidelity at input amplitudes greater than 80pA. However in the presence of the inhibitory commissural connection (Fig. 7A, continuous lines) there is a much more precipitous loss of asynchrony and generally poorer population response fidelity, because the closed-loop inhibitory system tends to promote the synchronization of neuron firing through the timing of its inhibitory inputs to the MVN neurons. By contrast in the Model 3 configuration, where asynchrony and response fidelity in the isolated MVNs are more robust over the entire amplitude range (Fig. 6B, dashed lines), the addition of a commissural inhibitory connection results in only a small reduction in asynchrony (Fig. 7B) as the synchronizing tendency is counteracted by the diffusive noise and pacemaker currents. As they are able to resist dramatic synchronization, the Model 3 neurons are able to exploit the differential amplification offered by the commissural inhibitory connection. This increases in fidelity at all amplitudes, particularly at small input amplitudes where signal to noise ratio is lowest and the amplification is most beneficial. A similar improvement of population response fidelity is seen for all frequencies (0.5-20Hz) tested in Model 3 neurons connected by an inhibitory commissural connection.

## 6. Discussion

### 6.1 Population asynchrony and signal transmission fidelity

In this study we have investigated the importance of asynchronous firing in a population of simulated neurons for the fidelity of signal transmission over a range of input amplitudes and frequencies, using the mammalian VOR pathway as an exemplar model system in which fidelity of brainstem MVN neurons is critical for accurate gaze stabilization. Our findings show that asynchrony in population activity, due to either diffusive noise inputs or the intrinsic, spontaneous activity of MVN neurons, is effective in maintaining a high fidelity population response over a wide operating range. In particular in the absence of both diffusive noise and pacemaker activity, the simulated MVN neurons show a strong tendency to synchronize in response to common input signals of moderate frequencies and amplitudes so that their signal transmission capacity is limited to a small range of low-frequency, medium-amplitude inputs. The presence of either diffusive noise or independent pacemaker currents in the individual MVN neurons results in a marked improvement in the operating range over which the population response is modulated with high fidelity, as they counter the MVN neurons' tendency to synchronize with each other and with phase lock with the input signal. While the addition of either diffusive noise or pacemaker activity improves signal transmission fidelity, optimal performance extending to higher input amplitudes and frequencies is obtained in a model where moderate levels of both diffusive noise and pacemaker currents are present (Fig. 5). Further increases in either the diffusive noise or the strength of pacemaker currents beyond optimal levels results in a deterioration of population response fidelity because this increases stochastic, non-input related spiking in the MVN neurons (Fig. 5). Moderate levels of both diffusive noise and pacemaker currents appear to act synergistically to generate population asynchrony and optimal response fidelity, without either one being large enough to add excessive stochastic firing.

Interestingly the values of diffusive noise and pacemaker activity which yield optimal fidelity of biologically relevant signal transmission in the simulated MVN neurons are similar to those which give a good approximation of the mean firing rate and coefficient of variation of MVN neurons *in vivo* (Fig. 6). This correspondence, despite the approximations and assumptions in our models, suggests that both diffusive noise and pacemaker-current heterogeneity are likely to be functionally important in maintaining the asynchrony and

population response behaviour of MVN neurons *in vivo,* and that these are broadly tuned to yield optimal fidelity.

These findings are in line with previous theoretical work in which diffusive noise was used to maintenance of asynchrony among spiking neurons (Knight, 1972; Gerstner, 2000; van Rossum et al., 2002). Heterogeneity amongst neurons was shown to have a similar effect on synchrony (Masuda and Aihara 2003; Masuda et al, 2005). Here we find that combining both is optimal to achieve a short-latency, high fidelity encoding of a common input signal in a population-rate code. Such signal transmission characteristics are highly appropriate for the mammalian VOR, which is characterised by high fidelity, phase aligned eye-movement response with near unity gain at up to 20Hz for voluntary and externally applied head on body rotations (Huterer & Cullen 2002) and beyond 20Hz for externally applied whole body rotations (Ramachandran & Lisberger 2005). This performance is in marked contrast, however, with electrophysiological properties of single MVN neurons. The frequency range over which individual MVN cells are able to respond to sinusoidal current injection without phase-locking is limited to about 10 -12 Hz, and at the higher frequencies only for very small input current amplitudes (du Lac and Lisberger 1995; Av-Ron and Vidal 1999; Ris et al., 2001). Although these studies are based on avian and rodent cell types, our own simulations indicate that in the absence of noise primate neurons are also vulnerable to phase locking and synchronization at higher frequencies and amplitudes (Fig. 3A).

On the basis of our present analysis, we suggest that the necessary wide frequency-response of the hVOR system is therefore not achieved by firing rate encoding of head velocity at the single-neuron level, but by the population-rate response of the asynchronously firing MVN neurons. This is consistent with a convergent innervation of abducens motoneurons by hVOR MVN neurons, so that each abducens motoneuron receives inputs from many MVN neurons. Abducens neurons are therefore well positioned to derive the integrated population response of the MVN cells.

### 6.2 Intrinsic excitability of MVN neurons

Our results suggest a novel biologically plausible role for the intrinsic, pacemaker-driven spontaneous activity of these neurons that has been extensively characterised in slice preparations of the MVN *in vitro.* See (Straka et al 2005) for a review. This interpretation predicts that multi-cellular recordings of MVN cells in vivo should observe asynchronous

activity and that pharmacological blockade of pacemaker activity should dramatically degrade VOR performance. It is notable that other neuron types also concerned with vestibular-related signals including prepositus hypoglossi neurons (Serafin et al., 1996b), and nucleus gigantocellularis neurons (Serafin, Vidal and Muhlethaler 1996a), have intrinsic membrane excitability and an *in vitro* spontaneous discharge analogous to that of MVN neurons (Straka et al 2005). Thus the ability to generate spontaneous intrinsic spiking activity, through the expression of pacemaker membrane conductances in individual neurons, may be a useful functional adaptation that promotes population asynchrony and a high fidelity population response beyond that achieved by means of diffusive noise alone, appropriate for VOR dynamics over a wide operating range.

**6.3 Potential functional role of subtypes of MVN neurons**

In this study we modelled a population of generic neurons, rather than attempt to model more accurately the different ionic conductances of Type A and Type B MVN neurons (Serafin et al., 1991; Johnston et al., 1994; Cartwright et al., 1999, 2003). It has been proposed that differences in the active membrane conductances of Type A and Type B neurons may underlie frequency-specific tuning or resonance in the responsiveness of each of these subtypes (Ris et al., 2001, Straka et al, 2005). This proposition is compatible with our analysis. Since both Type A and Type B cells are spontaneously active and discharge at broadly similar firing rates in slice preparations *in vitro,* the above findings on population response behaviour are likely to apply to both cell types. Indeed, it is an implicit corollary of the frequency-selective tuning of subtypes of MVN neurons (Straka et al, 2005), that the vestibular signal be encoded as a population response, rather than in the firing rate of individual neurons, in order to generate the required VOR performance over a wide frequency range.

Except for the comissural inhibitory connection, our study used only a single simple pathway. Other studies have tried to explain the detailed behavioural idiosyncrasies of the mammalian VOR in terms of parallel pathways. For example, it has been suggested suggests that the VOR is implemented by two parallel pathways. Ramachandran & Lisberger (2005, 2006) propose one fixed path, and one plastic path which can adapt to deal with changes in the lens or eye plant. Minor et al (1999) propose one linear path and one non-linear path.

Such parallel path proposals are also compatible with our framework as either or both pathways could be instantiated by a population rate code such as we describe.

### 6.4 MVN population asynchrony and the vestibular commissural inhibitory system

A prominent feature of the architecture of the VOR network in mammals is the reciprocal inhibitory commissure which links the MVN of the two sides (Fig. 1). We investigated the effects of linking two populations of simulated MVN neurons with a reciprocal inhibitory commissure, and investigated the role of neuronal firing asynchrony in shaping the population response of the linked MVNs. In the absence of diffusive noise and pacemaker current heterogeneity in the MVN neurons, the effects of reciprocal commissural inhibition were to drastically reduce the already limited fidelity of the individual MVNs (Model 0, Fig. 7A). This presumably reflects the amplification by the closed-loop commissural system of the differential head-velocity input signal applied to the bilateral MVN, which in the absence of the randomizing effects of diffusive noise and pacemaker currents, also potentiates the tendency of the two populations of MVN neurons to rapidly synchronize so that signal transmission fidelity collapses. Remarkably however, the addition of diffusive noise and pacemaker current heterogeneity to the MVN neurons leads to stable signal transmission and an improvement of population response fidelity (Model 3, Fig. 7B). Thus diffusive noise and pacemaker heterogeneity in MVN neurons, by counteracting neuronal synchronisation, enable the hVOR system to exploit differential amplification of the vestibular input signal by the commissural inhibitory system while maintaining population response fidelity over the required wide operating range. This further supports our proposed account of the high performance of the hVOR i*n vivo* and of the role of intrinsic pacemaker driven spontaneous activity of MVN neurons.

**References**


Arnold DB, Robinson DA (1997) The oculomotor integrator: testing of a neural network model. Exp Brain Res 113:57-74.

Av-Ron E, Vidal PP (1999) Intrinsic membrane properties and dynamics of medial vestibular neurons: a simulation. Biol Cybern 80: 383-392.

Burkitt AN, Clark GM (2001) Synchronization of the neural response to noisy periodic synaptic input. Neural Comput 13:2639-2672.

Cartwright AD, Curthoys IS (1996) A neural network simulation of the vestibular system: implications on the role of intervestibular nuclear coupling during vestibular compensation. Biol Cybern 75:485-493.

Cartwright AD, Curthoys IS, Gilchrist DP (1999) Testable predictions from realistic neural network simulations of vestibular compensation: integrating the behavioural and physiological data. Biol Cybern 81:73-87.

Cartwright AD, Gilchrist DP, Burgess AM, Curthoys IS (2003) A realistic neural-network simulation of both slow and quick phase components of the guinea pig VOR. Exp Brain Res 149:299-311.

Chen-Huang C, McCrea RA, Goldberg JM (1997) Contributions of regularly and irregularly discharging vestibular-nerve inputs to the discharge of central vestibular neurons in the alert squirrel monkey. Exp Brain Res 114:405-422.

Diesmann M, Gewaltig MO, Aertsen A (1999) Stable propagation of synchronous spiking in cortical neural networks. Nature 402:529–533.

du Lac S, Lisberger SG (1995) Cellular processing of temporal information in medial vestibular nucleus neurons. J Neurosci 15:8000-8010.

Graham BP, Dutia MB (2001) Cellular basis of vestibular compensation: analysis and modelling of the role of the commissural inhibitory system. Exp Brain Res 137:387-396.

Gerstner W (2000) Population dynamics of spiking neurons: fast transients, asynchronous state, and locking. Neural Comp 12:43–89.

Goldberg JM, Brown PB (1969) Response of binaural neurons of dog superior olivary complex to dichotic tonal stimuli: some physiological mechanisms of sound localization J Neurophysiol 32:613 - 636.

Huterer M, Cullen KE (2002) Vestibuloocular reflex dynamics during high-frequency and high-acceleration rotations of the head on body in rhesus monkey. J Neurophysiol 88:13-28.

Johnston AR, MacLeod NK, Dutia MB (1994) Ionic conductances contributing to spike repolarization and after- potentials in rat medial vestibular nucleus neurones. J Physiol (Lond) 481:61-77.

Knight BW (1972) Dynamics of encoding in a population of neurons. J Gen Physiol 59:734–766.

Masuda N, Aihara K (2003) Duality of rate coding and temporal coding in multilayered feedforward networks. Neural Comput 15:103-125.

Masuda N, Doiron B, Longtin A, Aihara K (2005) Coding of temporally varying signals in networks of spiking neurons with global delayed feedback. Neural Comput 17:2139-2175.

Minor LB, Lasker DM, Backous DD, Hullar TE (1999) Horizontal vestibuloocular reflex evoked by high-acceleration rotations in the squirrel monkey. I. Normal responses. J Neurophysiol 82:1254-1270.

Ramachandran R and Lisberger S (2005) Normal performance and expression of learning in the vestibulo-ocular reflex (VOR) at high frequencies. J. Neurophysiol. 93:2028-2038.

Ramachandran R and Lisberger, S (2006) Transformation of vestibular signals into motor commands in the vestibuloocular reflex pathways of monkeys. J Neurophysiol. 96:1061-1074.

Ris L, Godaux E (1998) Neuronal activity in the vestibular nuclei after contralateral or bilateral labyrinthectomy in the alert guinea pig. J. Neurophys. 80:2352-2367.

Ris L, Hachemaoui M, Vibert N, Godaux E, Vidal PP, Moore LE (2001) Resonance of spike discharge modulation in neurons of the guinea pig medial vestibular nucleus. J Neurophysiol 86:703-716.

Sekirnjak C and du Lac S (2002) Intrinsic firing dynamics of vestibular nucleus neurons. J Neurosci 22:2083-2095.

Serafin M, Vidal PP, Muhlethaler M (1996a) Electrophysiological study of nucleus gigantocellularis neurons in guinea-pig brainstem slices. Neuroscience 73:797-805.

Serafin M, de Waele C, Khateb A, Vidal PP, Muhlethaler M (1991) Medial vestibular nucleus in the guinea-pig. I. Intrinsic membrane properties in brainstem slices. Exp Brain Res 84:417-425.

Serafin M, Vibert N, De Waele C, Vidal PP, Muhlethaler M (1996b) Electrophysiological properties of nucleus prepositus hypoglossi neurons in guinea-pig brainstem slices. Soc Neurosci Abstr 22:263.262.

Straka H, Vibert N, Vidal PP, Moore LE, Dutia MB (2005) Intrinsic membrane properties of vertebrate vestibular neurons: function, development and plasticity. Prog Neurobiol 76:349-392.

van Rossum, MCW G.G. Turrigiano, and S.B. Nelson (2002), Fast propagation of firing rates through layered networks of neurons, J. Neurosc. 22, 1956-1966.

van Rossum, MCW (2001) Transient precision of integrate and fire neurons; effect of background activity and noise, J. Comput. Neurosc. 10, 303-310.

**Figures and Legends**

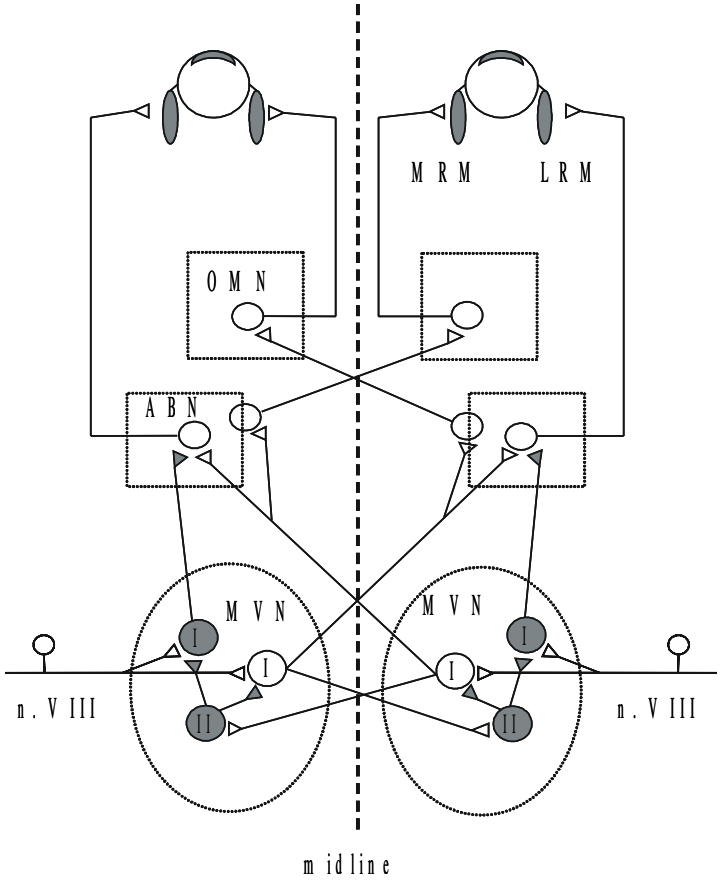


**Figure 1.** The basic hVOR network. Schematic diagram of the organisation of the medial vestibular nucleus (MVN) projections involved in mediating the horizontal vestibulo-ocular reflex (hVOR). Primary vestibular afferents from the horizontal semi-circular canals travel in the VIIIth cranial nerve (n. VIII) and synapse with second-order, 'Type I' MVN neurons in the brainstem. 'Type II' MVN neurons are inhibitory interneurons, which receive excitation from the contra-lateral MVN. Connections between the MVN neurons of the left and right sides form a reciprocal, commissural inhibitory system. Projections of the Type I MVN neurons to the abducens nucleus (ABN) and thence to the oculomotor nucleus (OMN) lead to the reflex activation of the medial and lateral rectus muscles (MRM and LRM respectively). The neurons actually simulated are Type I excitatory MVN neurons, which are the key middle neurons in the reflex arc. Shaded neurons and synapses are inhibitory.

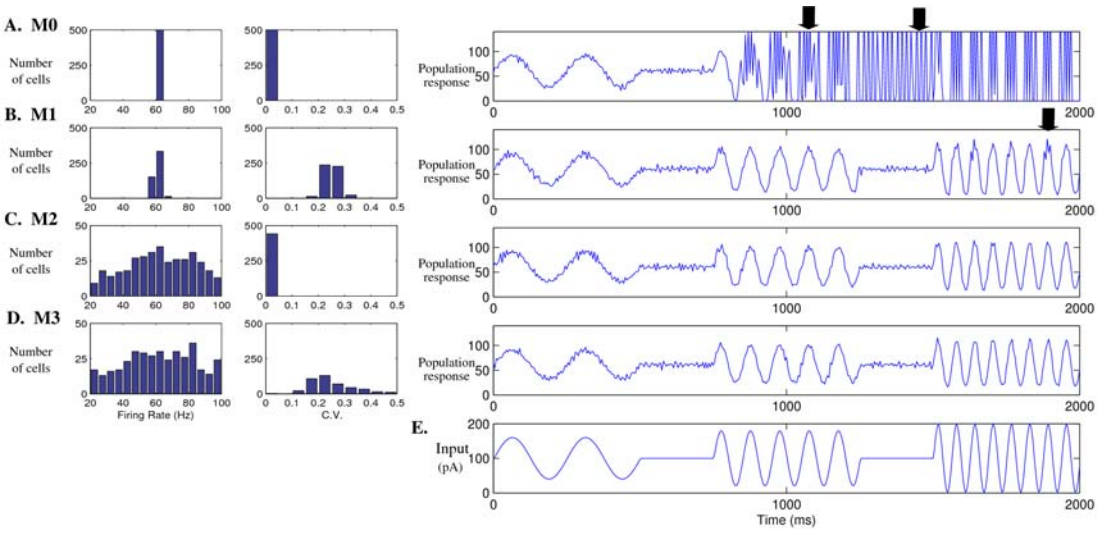


**Figure 2:** . Comparison of mean spike firing rate (*left*) and coefficient of variation of interspike intervals, CV (*middle*) of the population of simulated MVN neurons in each model variant, for the head-stationary resting input condition, *i(t)=0*. Population response to subsequent driven sinusoidal input at increasing frequencies and amplitudes (60pA, 4Hz; 80pA, 10Hz; 100pA, 16Hz) (*right*). The common input signal to all models *I(t)* is shown in (E). (A) In Model 0, where the MVN neurons received no diffusive noise input and had identical pacemaker currents, the neurons initially all fire regularly and at the same average rate. For moderate inputs the population activity in Model 0 begins to synchronize and the synchronous activity continues after the sinusoidal input has ended (arrows). (*B*) In Model 1, the addition of diffusive noise causes neurons to fire irregularly, but with similar average firing rates. It initially fires asynchronously and reflects the input well throughout the period in which Model 0 becomes synchronized. For the highest amplitude and frequency there is still a slight tendency to synchronize (arrow). (*C*) In Model 2, where the MVN neurons received no diffusive noise inputs but had heterogeneous pacemaker current amplitudes, the neurons exhibit a wide spread of mean rates across the population, but fire regularly. Good response is maintained throughout driven input. (*D*) In Model 3, where the MVN neurons received both diffusive noise inputs and had heterogeneous amplitudes of pacemaker currents, there is both a spread in mean rate and irregularity in firing. Good response is maintained throughout driven input.

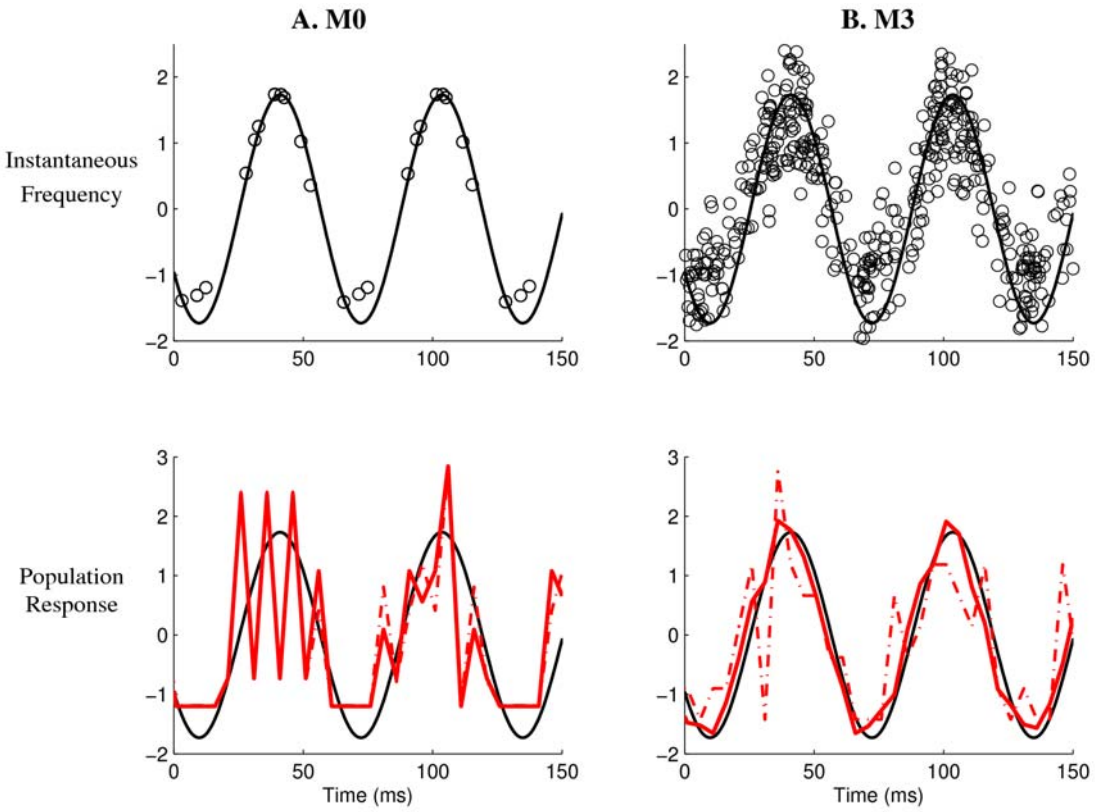


**Figure 3:** Detailed activity sample of cells in response to sinusoidal input and the resulting population response rate code. (A) Top: The synchrony (s=0.6) in spiking activity in Model 0 is clear with the overlapping, phase locked spike times (circles). As a result, the input (thin line) is therefore poorly represented by the instantaneous spike times. Similarly, the population response does not track the signal well(bottom). Furthermore, the population response does not improve when the number of cells is increased from 10 (broken line) to 500 (thick line). (B) The asynchrony (s=0.14) and noise in spiking activity in Model 3 spreads the spikes in time and around the input amplitude. The population response of 10 cells provides a coarse representation of the input, but the response of 500 cells is a good representation of the input. In the upper spike plots, only spikes from a random 50 cells are plotted to keep the Model 3 figure clear, however considering all 500 cells' spikes for Model 0 does not reveal any new unique spike times. Input is 16Hz frequency, 100pA amplitude.

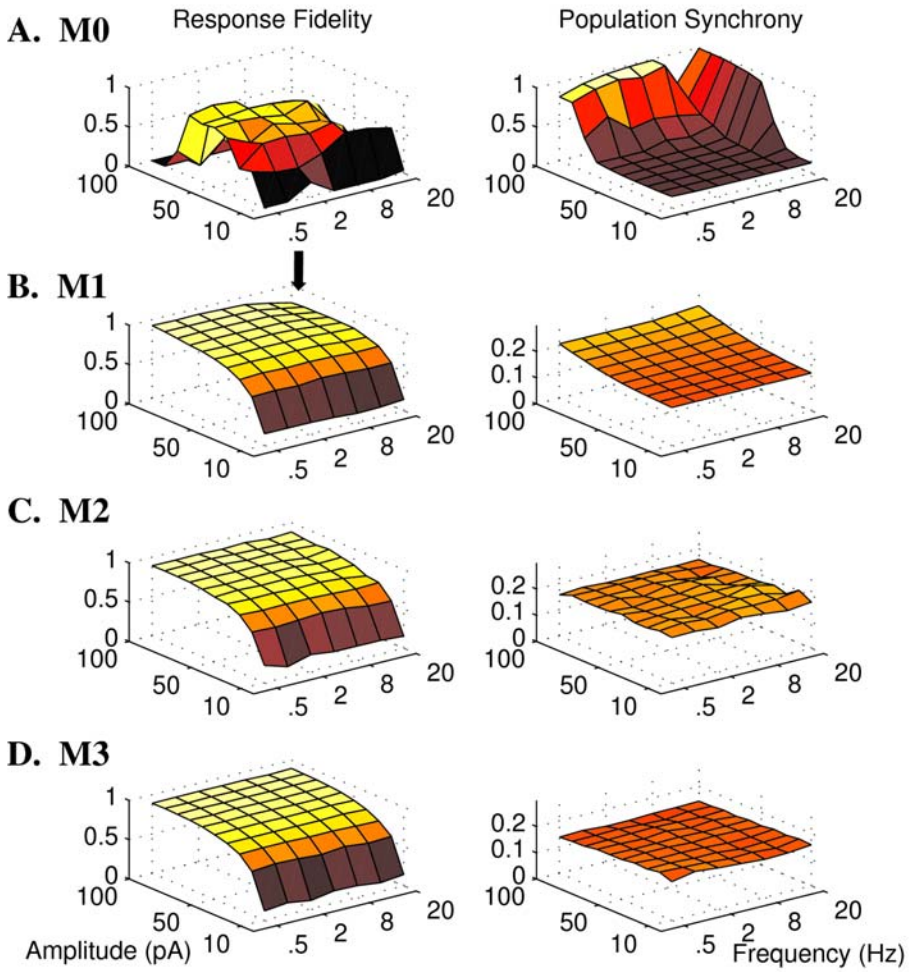


**Figure 4:** Dependence of response fidelity and population asynchrony on amplitude and frequency of signal input. Transmission fidelity *(left)* and population asynchrony *(right)* for model variants in response to a sinusoidal vestibular input *i(t)* of varying amplitude and frequency. Y-axes: amplitude of periodic input *i(t)*. X-axes: frequency of periodic input. (A) For Model 0 (homogeneous, noiseless neurons) the synchrony is high and the population response fidelity poor, particularly at the highest amplitudes and frequencies. (B) Model 1 (homogeneous neurons with diffusive noise), fidelity falls off at higher frequencies and amplitudes (arrow). In (C) Model 2 (heterogeneous neurons with no diffusive noise input), and (D) Model 3 (heterogeneous neurons with diffusive noise input), high fidelity and asynchrony are maintained across the parameter space. The data shown are averages for each simulation over 6s of sinusoidal driven input after settling.

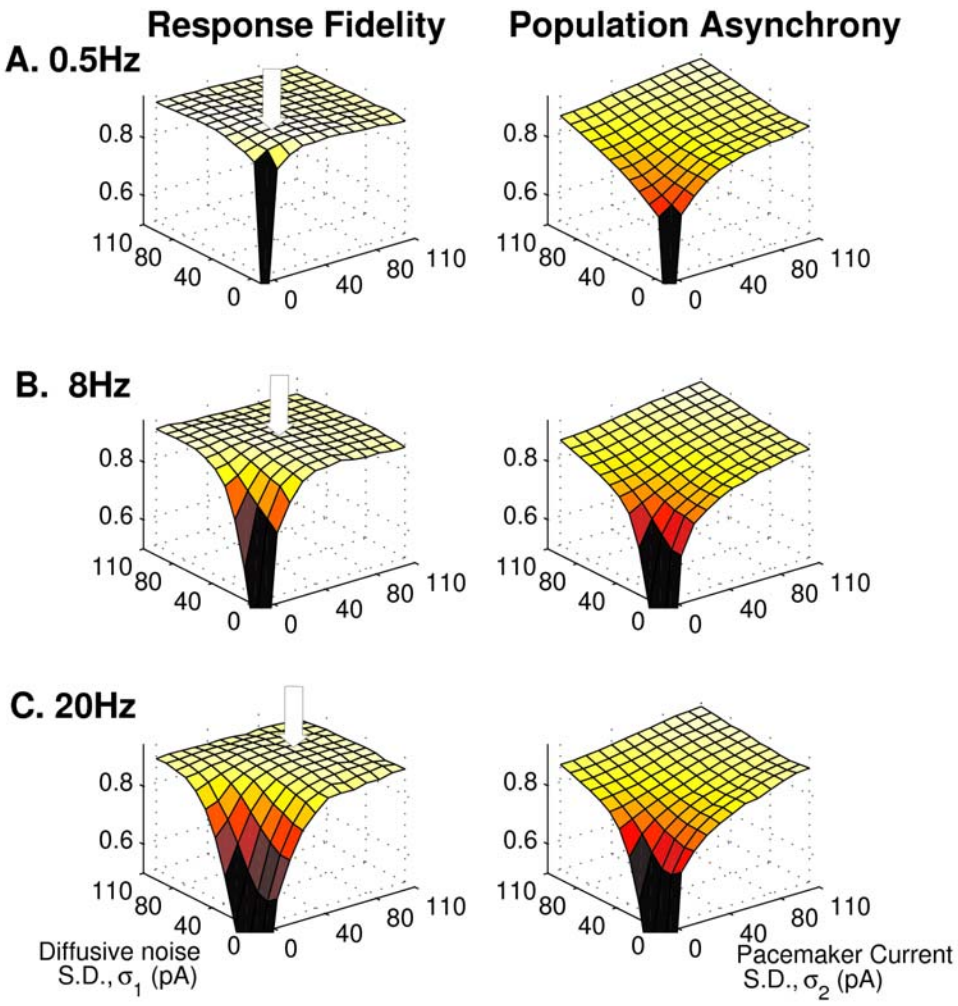


**Figure 5:** Dependence of response fidelity and population asynchrony on diffusive noise inputs and pacemaker currents. X-axes: diffusive noise standard deviation, $\sigma_1$. Y-axes: pacemaker current amplitude standard deviation, $\sigma_2$. *(A – C)* fidelity and asynchrony for signal input frequencies of 0.5, 8 and 20 Hz respectively. Asynchrony and fidelity increase rapidly from the origin with small additions of diffusive noise or pacemaker currents in all three cases. In each case moderate levels of diffusive noise and pacemaker current heterogeneity yield optimal response fidelity; increases in either parameter beyond these values lead to an increase in asynchrony and a decline in fidelity. For higher input frequencies, peak response fidelity is achieved at higher values of diffusive noise and pacemaker current heterogeneity (arrows, left column). Each point shown is the result averaged over five independent simulations, each of 2s length with the corresponding parameters $\sigma_1$,$\sigma_2$ and driven sinusoidal input of 100pA amplitude.

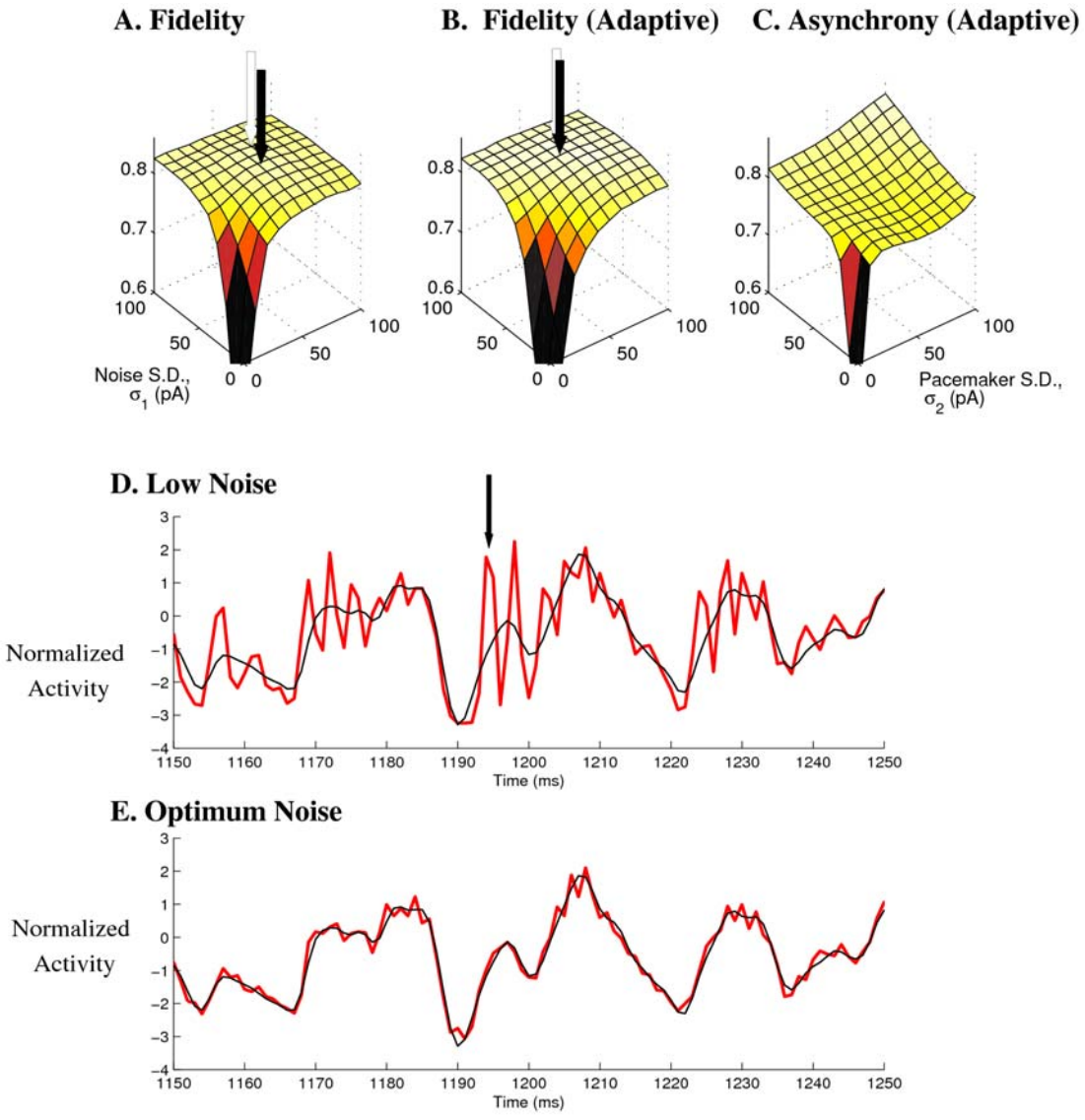


**Figure 6:** Response to multiple-frequency biologically relevant inputs suggests the diffusive noise and pacemaker parameters are tuned for optimal performance *in vivo.* Simple integrate and fire neurons (A), neurons with post inhibitory rebound firing and firing rate adaptation (B-E). Dependence of fidelity (A,B) and asynchrony (C) on diffusive noise and pacemaker currents using multiple-frequency input signals. Peak fidelity (black arrows) is obtained using parameters (A; $\sigma_1$=50pA, $\sigma_2$=50pA, B; $\sigma_1$=60pA, $\sigma_2$=50pA) that are very close to those which produce best fit to firing rate standard deviation and inter-spike interval coefficient of variation of MVN neurons *in vivo* (A,B; white arrows, $\sigma_1$=70pA, $\sigma_2$=60pA). (D) Sample from of normalized population firing activity (thick line) in response to multiple-frequency vestibular input *i(t)* (thin line), for a model MVN using low values for diffusive noise variance and pacemaker current heterogeneity ($\sigma_1$=10pA, $\sigma_2$=10pA). Arrows indicate

bursts of synchronous firing which are followed by refractory effects that markedly impair the fidelity with which the population activity follows the input signal. (E), The optimal values found for diffusive noise variance and pacemaker current heterogeneity yield a population response which follows the input signal with highest fidelity.

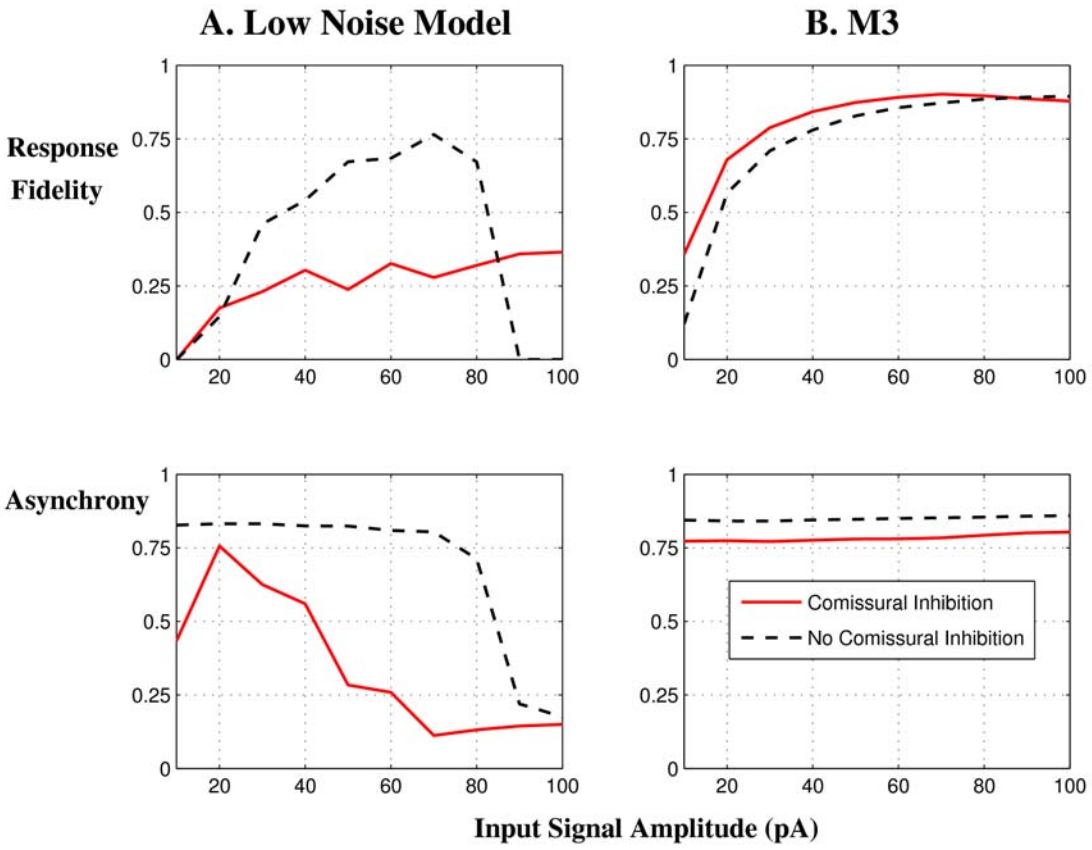


**Figure 7:** Effects of commissural inhibition on population asynchrony and response fidelity in a bilateral, reciprocally connected model containing two MVNs. (A), Low noise model with $\sigma_I = 5pA$, shows a loss of fidelity and asynchrony with input amplitudes larger than about 80 pA (dashed lines). When two Model 0 configuration MVNs are connected by a reciprocal commissural inhibitory system, there is a marked deterioration of fidelity and asynchrony (solid lines). (B), Model 3, with heterogeneous neurons and diffusive noise, maintains high fidelity and asynchrony for all input amplitudes, in both the isolated and commissurally connected simulations. In the presence of commissural inhibition, asynchrony is maintained and differential amplification provided by the commissural system yields a higher fidelity than in the isolated Model 3 MVN.